The Astrophysical Journal, 627:711–720, 2005 July 10
© 2005. The American Astronomical Society. All rights reserved. Printed in U.S.A.

CHANDRA OBSERVATIONS OF NGC 4261 (3C 270): REVEALING THE JET AND HIDDEN ACTIVE GALACTIC NUCLEUS IN A TYPE 2 LINER

A. Zezas
Harvard-Smithsonian Center for Astrophysics, 60 Garden Street, Cambridge, MA 02138

M. Birkinshaw and D. M. Worrall
Department of Physics, University of Bristol, Tyndall Avenue, Bristol BS8 1TL, UK

A. Peters
Department of Physics, University of Washington, Box 351580, Seattle, WA 98195-1580

and

G. Fabbiano
Harvard-Smithsonian Center for Astrophysics, 60 Garden Street, Cambridge, MA 02138
Received 2003 June 9; accepted 2005 February 17

ABSTRACT

We present results from a *Chandra* ACIS-S observation of the type 2 low-ionization nuclear emission-line region (LINER) radio galaxy NGC 4261 (3C 270). The X-ray data show that this galaxy hosts a heavily obscured ($N_{\rm H} \sim 8\times10^{22}$ cm^{-2}) active galactic nucleus (AGN) with an intrinsic luminosity of 2.4×10^{41} ergs s^{-1}, which dominates the energy output of the nucleus but is much less than the Eddington luminosity of its central massive black hole. The multiwavelength properties of this component are consistent with either radiatively inefficient accretion flows or emission from the inner part of a jet within 20 mas (3.4 pc) from the nucleus. A softer, unobscured power-law component, which we identify as synchrotron X-ray emission related to the unobscured part of the inner jet, produces ~10% of the 0.1–10.0 keV emission from the nucleus and is likely to be associated with the arcsecond-scale optical/UV emission measured with the *Hubble Space Telescope* (*HST*). These results indicate that the energy source of some type 2 LINERs could be a heavily obscured AGN, when obscuration of the ionizing continuum might be responsible for the low ionization state of the line-emitting gas.

Subject headings: galaxies: active — galaxies: elliptical and lenticular, cD — galaxies: individual (NGC 4261, 3C 270) — galaxies: nuclei — X-rays: galaxies

Online material: color figures

1. INTRODUCTION

The nature of low-ionization nuclear emission-line regions (LINERs) has been a matter of debate ever since their identification as a class of active galactic nuclei (AGNs) by Heckman (1980). The detection of broad emission lines in some LINERs in either direct (see, e.g., Ho et al. 1997a, 1997b) or scattered light (see, e.g., Barth et al. 1999) suggests that the energy source of these "type 1" LINERs is accretion onto a supermassive black hole. However, the nature of the central engine in "type 2" LINERs, which do not exhibit broad lines in their optical spectra, is still unknown. An intriguing case is that of type 2 LINERs that exhibit radio jets and lobes (indicating AGN activity) and yet have optical spectra that do not show any direct evidence for AGN activity. An example is NGC 4261. Possible scenarios for the energy source in these LINERs, as reviewed in Filippenko (1996), include massive stars (see, e.g., Filippenko & Terlevich 1992), evolved starbursts (see, e.g., Taniguchi et al. 2000; Alonso-Herrero et al. 2000), highly obscured AGNs (Imanishi et al. 2001), and shock excitation (see, e.g., Dopita et al. 1996, 1997). LINERs show relatively weak UV emission. This is consistent with star formation (Maoz et al. 1995). Terashima et al. (2000), after studying a sample of type 2 LINERs with the *ASCA* X-ray observatory, also reached the conclusion that in most cases their X-ray emission could be related to star formation. X-ray observations are a powerful tool in the investigation of these scenarios because X-rays can penetrate obscuring material of high column densities.

NGC 4261 is an E2 elliptical galaxy located at a distance of 35.1 Mpc, with a nucleus classified as a type 2 LINER based on high-quality optical spectra (Ho et al. 1997b). Its position on the diagnostic diagrams of Kewley et al. (2001) suggests that the optical emission is due either to a hard photoionizing field with low ionization parameter or to emission by fast shocks, without an ionizing precursor, propagating in a gas-poor environment. *Hubble Space Telescope* (*HST*) WFPC2 observations (Jaffe et al. 1993) showed a bright nuclear optical source surrounded by a disk of gas and dust, suggesting large concentrations of gas in this region, which is unexpected in the shock scenario. Recent kinematic studies of the nuclear ionized gas find a nuclear black hole mass of $(4.9 \pm 1.0)\times10^8\ M_\odot$ (Ferrarese et al. 1996).

Apart from the dynamical evidence for a supermassive black hole in NGC 4261, the strongest indication for the existence of an AGN in this galaxy comes from radio observations: NGC 4261 is an FR-I radio galaxy featuring two prominent radio jets feeding low-power lobes (see, e.g., Birkinshaw & Davies 1985). High-resolution VLBI observations probed the jet to subparsec scales (Jones et al. 2000), and Jones et al. (2001) report a detection of an accretion disk at a scale of 0.2 pc from its shadow on the jet. A jetlike feature in the nuclear region of NGC 4261 has also been detected in UV images obtained with *HST* STIS and has been interpreted either as synchrotron emission from the jet or as scattered nuclear emission (Chiaberge et al. 2003). The multiwavelength parameters of the nucleus are presented in Table 1.

TABLE 1
PROPERTIES OF THE NUCLEUS

Parameter	Value	References
R.A. (J2000)	$12^h19^m23^s.22$	
Decl. (J2000)	$+5°49'29''.70$	
Distance	35.1 Mpc	Ho et al. (1997b)
M_{BH}	$(4.9 \pm 1.0) \times 10^8\ M_\odot$	Ferrarese et al. (1996)
f_{rad} (5.0 GHz)	293 mJy	Worrall & Birkinshaw (1994)
$f_{H\alpha}$	1.5×10^{-14} ergs cm^{-2} s^{-1}	Ho et al. (1997b)
f_X[a] (0.1–2.0 keV)	1.6 (7.5)	
L_X[b] (0.1–2.0 keV)	2.4 (13.9)	
f_X[a] (2.0–10.0 keV)	6.97 (10.6)	
L_X[b] (2.0–10.0 keV)	10.3 (15.6)	

NOTE.—The X-ray data are from this work.
[a] Observed (absorption-corrected) flux in units of 10^{-13} ergs cm^{-2} s^{-1}, based on model 5 (Table 2).
[b] Observed (absorption-corrected) luminosity in units of 10^{40} ergs s^{-1}, based on model 5 and for a distance of 35.1 Mpc.

Previous X-ray observations of NGC 4261 with the *Einstein* IPC revealed a moderately luminous nucleus ($L_{X,(0.2-4.0\ keV)} = 1.6 \times 10^{41}$ ergs s^{-1}; Fabbiano et al. 1992). Spectral fits of *ROSAT* PSPC data showed that a two-component model consisting of a thermal plasma ($kT \sim 0.6$ keV) and a poorly constrained power law ($\Gamma \sim 1.7$) without any excess absorption gives a good representation of its soft X-ray spectrum (Worrall & Birkinshaw 1994). Spatial analysis associated the power-law emission with the nucleus, and the thermal emission with the galaxy-scale atmosphere. Broadband spectroscopy with *ASCA*, which can better constrain the hard emission, shows a relatively flat power-law index ($\Gamma = 1.45$; Matsumoto et al. 2001; Terashima et al. 2002). However, the large beam of *ASCA* and the restricted energy band of *ROSAT* hamper the investigation of the X-ray components, since the data confuse emission from the nucleus, the radio jets, and the host galaxy. Indeed, observations of other LINERs with *Chandra* indicate that the nucleus does not always dominate the X-ray emission of the host galaxy (see, e.g., Ho et al. 2001; Eracleous et al. 2002; Pellegrini et al. 2002; Georgantopoulos et al. 2002; A. Zezas et al. 2005, in preparation). Recent *XMM-Newton* observations of NGC 4261 showed that its X-ray spectrum could be fitted with an absorbed, relatively flat power law ($\Gamma \sim 1.4$) and a soft thermal component (Sambruna et al. 2003). The same data also showed evidence for short-term variability and an Fe K line, which the authors attribute to the inner part of the jet and the accretion flow, respectively.

We observed NGC 4261 with *Chandra* (Weisskopf et al. 2000), whose subarcsecond resolution allows us to separate the X-ray emission components. A first analysis of these *Chandra* data by Chiaberge et al. (2003) showed a flat overall X-ray spectrum with relatively high column density, which, as they pointed out, appears to be inconsistent with the detection of UV emission from the nucleus. More recently, a combined *XMM-Newton*/*Chandra* study of NGC 4261 led to the conclusion that the X-ray continuum is produced by the accretion flow (Gliozzi et al. 2003). In this paper we present an alternative interpretation of the X-ray continuum, favoring a jet model for at least the soft X-ray emission, in the light of the spectral parameters of the X-ray components and their relation to the radio and optical emission. In § 2 we present results from the imaging and spectral analysis of the *Chandra* data, while in § 3 we discuss different models for the nature of the nucleus and the implications of these results for the LINER phenomenon.

2. OBSERVATIONS AND DATA ANALYSIS

NGC 4261 was observed for 35 ks with the back-illuminated S3 CCD of the Advanced CCD Imaging Spectrometer (ACIS; Garmire 1997) on board the *Chandra X-Ray Observatory*. The observation was performed in 1/2 subarray mode, which gives a frame time of 1.8 s in order to limit pile-up to less than 10%, based on the strength of the emission component, which was unresolved with the *ROSAT* PSPC (Worrall & Birkinshaw 1994). The *Chandra* nuclear count rate of 0.07 counts s^{-1} corresponds to a pile-up of $<10\%$ for the flattest spectrum consistent with the data, which is tolerable.

For our analysis we used the type 2 event (evt2) files after applying the gain maps of CALDB version 2.12. These files include only events of status 0, and grades 0, 2, 3, 4, and 6. A search for periods of enhanced background showed that the S3 CCD background throughout the observation was slightly higher than nominal (although this might be due to diffuse emission associated with the galaxy or an extended group; Davis et al. 1995) but did not exhibit any flares. In the following analysis we use data in the 0.3–7.0 keV band because of the calibration uncertainties at lower energies and the enhanced contribution of the particle background at high energies. The analysis was performed with the *Chandra* Interactive Analysis of Observations (CIAO) version 2.2.1 tool suite.

2.1. *Imaging Analysis*

To investigate the emission of the nuclear region of NGC 4261, we created images in soft (0.3–2.0 keV) and hard (2.0–4.0 keV) bands for the central $1'.5$ of the galaxy (which corresponds to a physical size of 15.3 kpc; the D_{25} radius of the galaxy is $4'$; de Vaucouleurs et al. 1991). In order to show low surface brightness and small-scale features, these images were lightly smoothed using a top-hat smoothing kernel with a width of 2.5 pixels ($\sim 1''.25$). Both images together with an *HST* WFPC2 *R*-band image of the nucleus are shown in Figure 1. From this figure we see that there is a significant amount of diffuse soft emission along with a strong pointlike nuclear source, which is visible in both bands but dominates in the hard band.

A ridge of extended emission along the east-west direction is clearly seen in both bands. This is associated with the radio jet and will be discussed in detail elsewhere. In order to measure the extent of the jet in the X-ray band, we created a model of the extended nuclear emission in the 0.3–5.0 keV band by fitting a

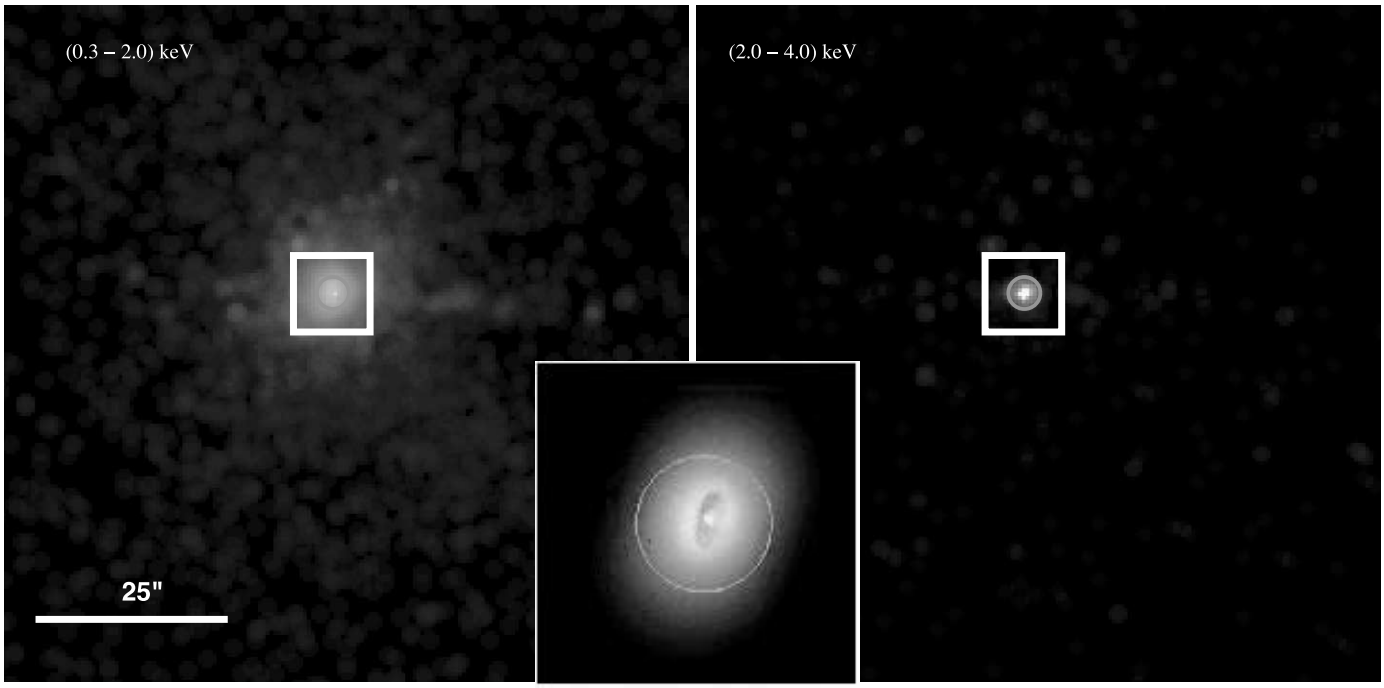

FIG. 1.—Soft-band (0.3–2.0 keV; *left*) and hard-band (2.0–4.0 keV; *right*) lightly smoothed images of the nuclear region of NGC 4261 (in both images, north is up and east is to the left). An *R*-band *HST* WFPC2 image of the nucleus with the same orientation as the X-ray image is shown in the insert. The region of the insert is indicated by the white square on the X-ray images. The white circle shows the extraction region for the nuclear spectrum. The physical size of the X-ray images is 15.3 kpc × 15.3 kpc (1′.5 × 1′.5). [*See the electronic edition of the Journal for a color version of this figure*.]

two-dimensional elliptical model to the smoothed image. Then we subtracted this model from the raw data. The resulting image is presented in Figure 2. For reference in the same image, we also show contours from a VLA[1] *C*-band (6 cm) image with a resolution of 2″.3 × 1″.8.

To study the spatial extent of the nuclear emission, we extracted radial profiles centered on the nucleus from unsmoothed soft-band (0.6–1.0 keV) and hard-band (4.0–8.0 keV) images, and we compared them with point-source models created with the *mkpsf* tool for energies of 1.4 and 4.5 keV, respectively. The energy ranges were chosen with the expectation of emphasizing the thermal gas (soft band) and the nuclear emission (hard band), based on the results from the spectral fitting (§ 2.2). The contribution of the jet component in these two bands is small compared to the nuclear and the thermal gas components. A comparison between the point-source models and the measured profiles shows that the soft emission is clearly extended, while the hard emission is almost pointlike (Fig. 3). A fit of the profile of the soft emission with a Gaussian gives a deconvolved FWHM of 4″.9. There is no offset in the centroid of the emission between the soft and the hard bands.

In order to determine the absolute astrometric accuracy of this observation, we searched the USNO-A2.0 star catalog[2] and the 2MASS catalog for sources within the active field of view of the ACIS-S3 CCD. We found two such sources with an offset from their X-ray counterparts less than 0″.5 and not in the same direction. Therefore we conclude that the absolute astrometry of these observations is good to within 0″.5, in accordance with estimates from the calibration team.[3] Moreover, we find excellent agreement between the position of the nucleus and the multiwavelength astrometric data given in Ferrarese et al. (1996), showing that the X-ray data trace the same nuclear source as is seen in other energy bands.

We confirmed this by analyzing archival *HST* WFPC2 *R*-band (F675W filter) data, following the standard procedures described in Biretta et al. (1997). We chose the *R*-band data since they are less affected by extinction than UV data. After correcting for differences in the relative astrometry of the *Chandra* and *HST* images using two common sources, we found that the offset between the optical and the X-ray nucleus is ∼0″.20. This is within the spatial resolution of the X-ray data and therefore we

[1] The VLA is operated by the National Radio Astronomy Observatory, which is a facility of the National Science Foundation, operated under cooperative agreement by Associated Universities, Inc.

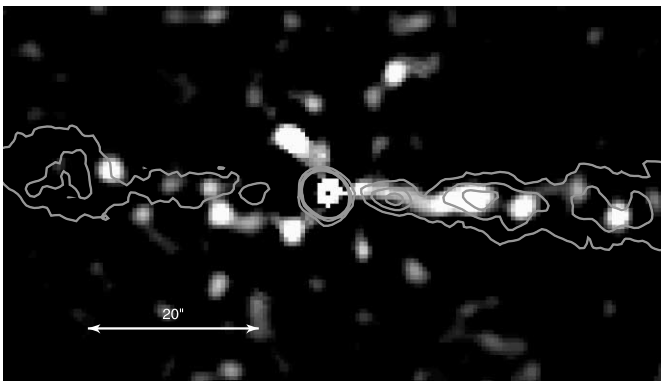

FIG. 2.—0.3–5.0 keV image after subtracting the diffuse component (see text for details). The contours correspond to radio emission from a 4.9 GHz VLA observation (2″.3 × 1″.8 beam; Birkinshaw & Davies 1985).

[2] See http://ftp.nofs.navy.mil/projects/pmm/index.html.
[3] See http://cxc.harvard.edu/cal/ASPECT/celmon/.

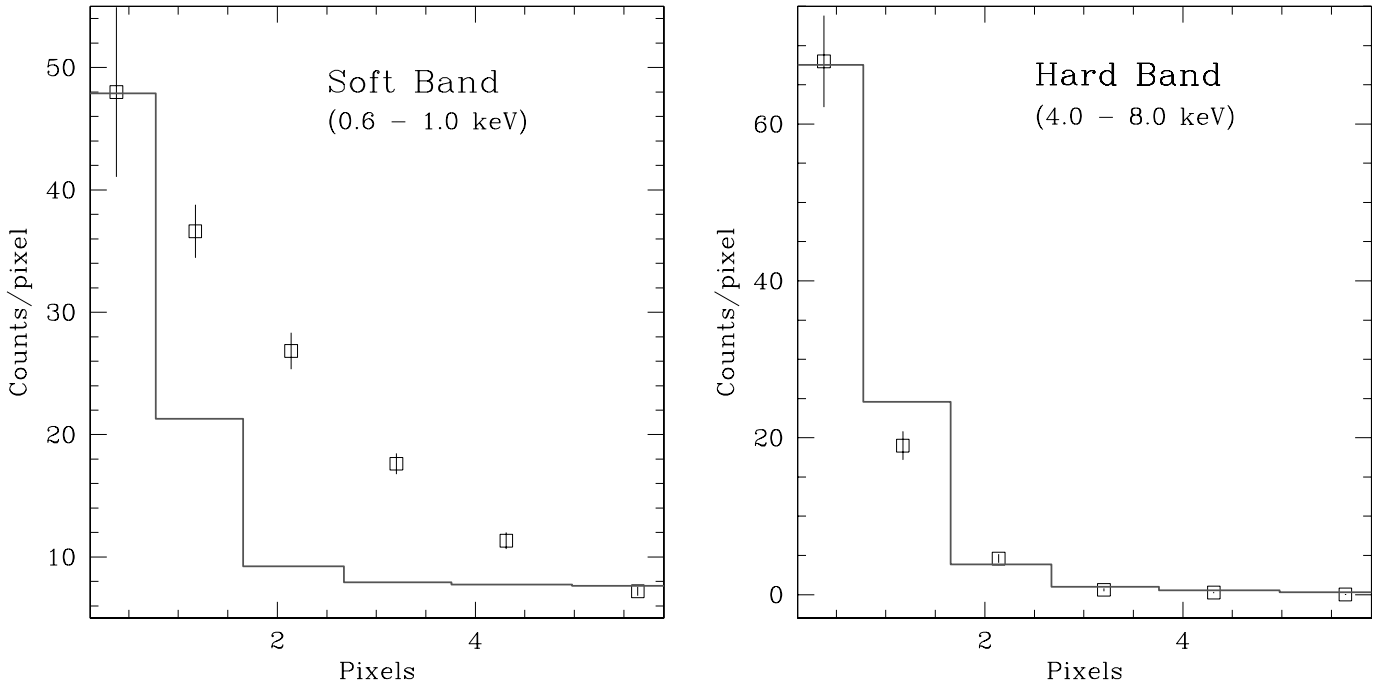

FIG. 3.—Comparison between the nuclear and point-source radial profiles in the soft (*left*) and hard (*right*) band. One pixel corresponds to 0.″49 or ~70 pc at the distance of the galaxy. [*See the electronic edition of the Journal for a color version of this figure.*]

conclude that the brightest X-ray source is associated with the optical nucleus to within an accuracy of ~0.″5. The X-ray parameters of the nucleus are presented in Table 1.

2.2. *Spectral Analysis*

We extracted the nuclear spectrum from a circular aperture of 2″ radius centered on the nucleus (shown as a white circle in Fig. 1). This extraction region encompasses 95% of the energy of a point source at 1.5 keV, and 90% of the energy at 6.5 keV, while its small size minimizes the contribution of the circumnuclear diffuse emission. A spectrum of the local background, accounting for the instrumental background as well as the contribution of the circumnuclear diffuse emission (which dominates in the soft band), was obtained from an annulus around the nucleus between $r_{\rm min} = 2.''8$ (~0.5 kpc) and $r_{\rm max} = 8.''8$ (1.5 kpc). Two pointlike sources lying within this background region were excluded. We detect a total of 2677 counts in the nuclear source aperture, 155 of which are estimated to be due to the local background. The nuclear spectrum was grouped to a minimum of 25 counts per bin before background subtraction, in order to apply χ^2 statistics. For the spectral analysis, we used the XSPEC version 11.1 package. The results of the spectral fits are presented in Table 2. We corrected for the time-dependent degradation of the ACIS sensitivity (see, e.g., Marshall et al. 2004) by using the ACISABS model in XSPEC. We also performed tests with ancillary response files (arf) created with CIAO version 3.0 (using CALDB ver. 2.26), and we found no difference within the uncertainties through changing the calibration and analysis technique.

Simple models such as an absorbed power law (PO; model 1) or absorbed Raymond-Smith thermal plasma (RS; Raymond & Smith 1977) gave unacceptable fits to the nuclear spectrum ($\chi^2_\nu > 10.0$). A combination of a thermal plasma and a power-law component (model 2) resulted in an improved fit at more than 99% confidence level (based on an *F*-test for two additional parameters; see, e.g., Bevington & Robinson 1992) but still with an unacceptable $\chi^2_\nu > 2.0$. The best-fit temperature for the thermal component was $kT = 0.41$ keV, and the slope of the power law was $\Gamma = -0.02$.[4] This very flat power law suggests that the hard component is either heavily absorbed or dominated by reflection (cf. Turner et al. 1997; Matt et al. 2000). However, including an absorber for the power law (model 3) did not improve the fit, and no additional absorbing column was required ($N_{\rm H} < 7.8\times10^{20}$ cm^{-2}).

Since from the imaging analysis we find that the X-ray jet extends to the nucleus, we attempted to model a jet-related component with a second power law, absorbed by a different column (model 4). This model gave an improved fit at more than 95% confidence level based on an *F*-test for three additional parameters. The best-fit slopes for the two power laws are $\Gamma_1 = 1.46$ and $\Gamma_2 = 2.25$, while their respective column densities were $N_{\rm H,1} = 8.13\times10^{22}$ cm^{-2} and $N_{\rm H,2} < 9.6\times10^{20}$ cm^{-2}. We also investigated the existence of an unresolved Fe Kα line at 6.4 keV (absorbed by the same column as the hard power law; model 5), which is usually a telltale signature of AGN activity (see, e.g., Nandra et al. 1997). The inclusion of this component slightly improved the χ^2 but not at a statistically significant level (30% probability of improvement in χ^2 by chance, based on an *F*-test). The new parameters for the continuum ($\Gamma_1 = 1.54^{+0.71}_{-0.39}$, $N_{\rm H,1} = 8.4^{+3.8}_{-3.0}\times10^{22}$ cm^{-2}, $\Gamma_2 = 2.25^{+0.52}_{-0.28}$, and $N_{\rm H,2} < 3.7\times10^{20}$ cm^{-2}) are consistent within the 1 σ errors with the parameters of the previous model (model 4). The equivalent width (EW) of the line with respect to the unabsorbed continuum of the power-law component is 260 eV (<590 eV at 90% confidence for three interesting parameters; Table 2). Our best-fit value is consistent with the EW of the Fe Kα line detected in the *XMM-Newton* spectrum of NGC 4261 (Sambruna et al. 2003). This best-fit model together with the observed spectrum is presented in Figure 4,

[4] As is demonstrated later in this section, the dependence of the derived spectral parameters on the abundance of the thermal components is small; therefore, all thermal components have solar abundances unless otherwise stated.

TABLE 2
FITTING RESULTS

Parameter	Model 1	Model 2	Model 3	Model 4	Model 5
Γ_1	$1.49^{+0.09}_{-0.1}$	$-0.02^{+0.07}_{-0.09}$	$0.03^{+0.12}_{-0.13}$	$1.46^{+0.67}_{-0.55}$	$1.54^{+0.71}_{-0.39}$
Norm$_1$[a]	$4.35^{+0.21}_{-0.22}$	$1.04^{+0.19}_{-0.15}$	$1.05^{+0.18}_{-0.16}$	$10.3^{+24.5}_{-8.0}$	$18.1^{+47.4}_{-12.1}$
Γ_2	...	...	...	$2.25^{+0.59}_{-0.06}$	$2.25^{+0.52}_{-0.28}$
Norm$_2$[a]	...	...	...	$2.4^{+0.96}_{-0.33}$	$2.4^{+0.95}_{-0.37}$
kT (keV)	...	$0.41^{+0.02}_{-0.03}$	$0.28^{+0.04}_{-0.03}$	$0.41^{+0.02}_{-0.02}$	$0.5^{+0.04}_{-0.04}$
Norm$_3$[b]	...	$5.68^{+0.33}_{-0.36}$	$5.68^{+0.36}_{-0.32}$	$4.15^{+0.36}_{-0.36}$	$4.15^{+0.37}_{-0.36}$
N_H (total)[d]	0.0 (<0.006)	0.058[c]	0.058[c]	0.058[c]	0.058[c]
$N_{H,1}$ (soft)[d]	...	...	<0.078	<0.034	<0.037
$N_{H,2}$ (hard)[d]	...	...	...	$8.13^{+3.15}_{-3.1}$	$8.37^{+3.83}_{-3.03}$
Energy (keV)	...	...	...	...	$6.38^{+0.07}_{-0.25}$
Equivalent width (eV)[e]	...	...	...	...	260 (<590)
χ^2 (dof)	951.2/69	152.9/68	152.9/67	83.7/64	80.5/62

NOTE.—Description of the models: model 1: Abs (PO); model 2: Abs (RS + PO); model 3: Abs (RS + Abs[PO]); model 4: Abs (RS + Abs[PO] + Abs[PO]); model 5: Abs (RS + Abs[PO] + Abs[PO + G3]). Abs: cold absorption (wabs model in XSPEC); RS: Raymond-Smith (Raymond & Smith 1977) thermal plasma; PO: power law; G: Gaussian line. All errors are at the 90% confidence level for one interesting parameter, unless otherwise stated.

[a] Norm$_1$, Norm$_2$: Normalization of the power-law components in units of 10^{-5} photons s^{-1} keV^{-1} cm^2 at 1 keV.

[b] Norm$_3$: Normalization of the thermal plasma component in units of $10^{-19} \int n^2 dV/4\pi D^2$ cm^{-5}, where D is the distance and n is the electron density.

[c] N_H fixed to the Galactic value.

[d] N_H, $N_{H,1}$, and $N_{H,2}$ are in units of 10^{22} cm^{-2}.

[e] Equivalent width of the Fe Kα line with respect to the hard power-law continuum errors have been calculated from the uncertainty in the line normalization for three interesting parameters (hard power-law slope and normalization, line normalization) and with the other model parameters fixed to their best-fit values.

and the contribution of the different spectral components to the 0.1–10.0 keV X-ray luminosity of NGC 4261 is given in Table 3.

Based on the emission measure of the thermal nuclear component within the 2″ (340 pc) extraction radius, and assuming an isothermal sphere, we estimate a gas density of 0.34 cm^{-3} within a radius of 0.32 kpc of the nucleus. This corresponds to a total mass of $1.6 \times 10^6\ M_\odot$ within the sphere and a cooling time of ~60 Myr.

Since the slopes of the two power-law components could be consistent within the errors, the double power-law model is phenomenologically similar to a partially covering absorber. Therefore, we fitted the data with a power law seen through a partially covering absorber and an additional thermal plasma component. The overall spectrum is seen through a neutral absorber with a column density fixed to the Galactic value along the line of sight. This model gives a fit of the same quality as the double power-law model. We find a best-fit photon index of $\Gamma = 1.37^{+0.53}_{-0.37}$, seen through an absorber with $N_H = 7.7^{+3.3}_{-2.7} \times 10^{22}$ cm^{-2}, and a covering factor of $0.92^{+0.04}_{-0.07}$. Similar values have also been reported by Gliozzi et al. (2003) from their fits to the *Chandra* and *XMM-Newton* spectra of NGC 4261.

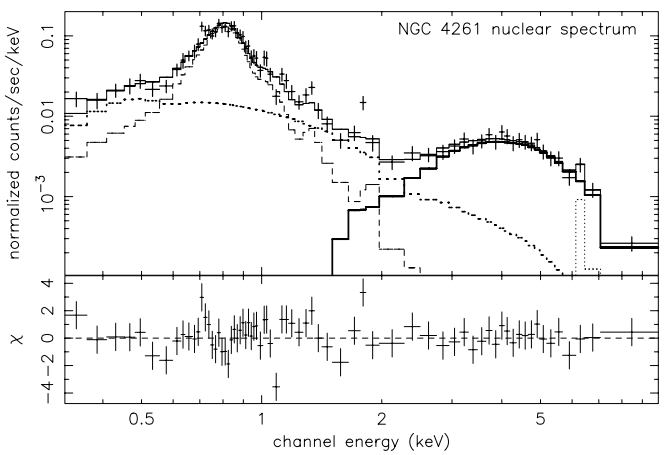

FIG. 4.—Best-fitting model of the nuclear spectrum (model 5 in Table 2) and the residuals in units of σ. The light dashed line shows the thermal component, the heavy line shows the power-law components (*solid for the hard, absorbed power law, and dotted for the soft, unabsorbed component*), and the light dotted line shows the Fe Kα line.

Since such a hard spectrum is also typical of an AGN with a strong reflection component (see, e.g., Matt et al. 2000), we replaced the hard power law in the last spectrum with a reflection model (PEXRAV model in XSPEC). This model gives the reflected spectrum from an illuminated slab of neutral material (Magdziarz & Zdziarski 1995). The incident spectrum is a power law, and the viewing angle is fixed at $\theta = 65°$ ($\cos\theta = 0.45$). Fits with the reflected and direct components free to vary resulted in a small contribution of the reflected component, making this model effectively indistinguishable from the previously presented double power-law model (model 5) but not improving the quality of the fit. Next we investigated the case for a pure reflection component. Again the quality of the fit was not improved over the power-law fits.

The results of the spectral fits showed evidence for a thermal component ($kT = 0.4$ keV; Table 2) in the nuclear spectrum, which most probably is associated with the circumnuclear diffuse emission (see, e.g., Fig. 1). We investigated the properties of the gas outside the core by extracting spectra from four annuli between 0.4 and 2.8 kpc from the nucleus. From these regions, we excluded any pointlike sources and jet emission. The background was taken from source-free regions in the outskirts of the galaxy. We used the PROJECT model in XSPEC to deproject the four spectra, fitted by an absorbed thermal plasma model with atomic hydrogen column density fixed to the Galactic line-of-sight value. The four models had the same abundance, which was free to vary. We find that there is no temperature gradient outside the core region (typical temperature ~0.6 keV) out to ~3.0 kpc from the nucleus, while the best-fit abundance was significantly

TABLE 3
CONTRIBUTION OF SPECTRAL COMPONENTS IN OVERALL EMISSION

COMPONENT	OBSERVED LUMINOSITY[a]		INTRINSIC LUMINOSITY[a]	
	0.1–2.0 keV	2.0–10.0 keV	0.1–2.0 keV	2.0–10.0 keV
Hard power law	0.2	92.6	95.1	145.8
Soft power law	8.3	6.3	21.3	6.3
Thermal Component	15.9	0.2	23.4	0.2
Fe Kα line	...	3.7	...	4.3
Total	24.4	102.8	139.8	156.5

NOTE.—Based on the spectral fits with model 5 (Table 2).
[a] Luminosity in units of 10^{39} ergs s^{-1}.

subsolar ($0.22^{+0.05}_{-0.03}$ $Z_\odot$). These values are similar to those measured with *ASCA* for other early-type galaxies (see, e.g., Matsushita et al. 2000).

However, Xu et al. (2002) find higher abundances (0.5–1.0 $Z_\odot$, depending on the element) based on high-resolution X-ray spectra of the elliptical galaxy NGC 4636. Moreover, studies of the diffuse emission in the Fornax A galaxy showed that a contaminating power-law component from an unresolved population of X-ray binaries (XRBs) may result in subsolar abundances in spectra fitted with a single thermal component (Kim & Fabbiano 2003). Therefore, we also fitted the spectrum of each annulus with a two-component model consisting of a thermal plasma (with abundance fixed to the solar value) and an absorbed power law (representing a population of unresolved XRBs). This model also gave a good fit for all four annuli. The overall absorbing column density was free to vary, but its lower limit was fixed to the Galactic value along the line of sight. The power-law component comprises <50% of the total 0.1–2.0 keV emission (corrected only for the foreground absorbing column) in any annulus, and within the uncertainties the fraction of the emission from the power law is consistent across all annuli (Fig. 5). The best-fit temperature of the thermal component is ~0.6 keV in all bins, slightly higher than but consistent with the temperature of the nuclear thermal component. The photon indices in all four annuli were similar within the errors and consistent with those of low-mass XRBs ($\Gamma \sim 1.7$–2.0; see, e.g., Irwin et al. 2003; Colbert et al. 2004) but steeper than the power law measured in the nuclear spectrum. Only in the two innermost annuli do we measure significant absorption for the power-law component; the first requires an absorption of 9.4×10^{21} cm^{-2} (although this is strongly correlated with the poorly constrained slope of the power law), while the second annulus requires a somewhat lower absorption ($N_{\rm H} \sim 1.6 \times 10^{21}$ cm^{-2}). The best-fit temperatures and photon indices for each bin are also presented in Figure 5.

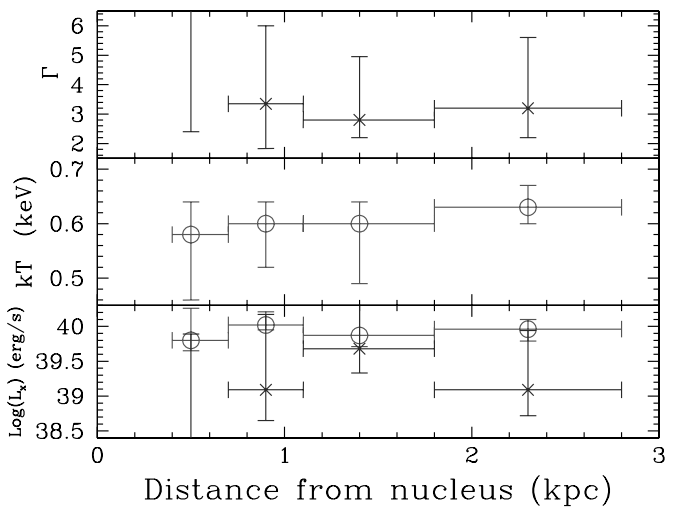

FIG. 5.—Spectral properties of the circumnuclear diffuse emission. The top panel shows the parameters of the absorbed power law, while the middle panel shows the temperature distribution (see text for details). The bottom panel shows the luminosity of each component in the 0.1–10.0 keV band (corrected only for foreground absorption) in units of ergs s^{-1}. Points shown by crosses correspond to the power-law component, and the points shown by circles correspond to the thermal component. The errors reflect the 1 σ uncertainties in the model normalizations and do not take into account uncertainties in any other spectral parameters. [*See the electronic edition of the Journal for a color version of this figure.*]

In order to assess the effect of a low-abundance thermal component in the spectral fits of the nuclear source, we repeated them by fixing the abundance of the Raymond-Smith model component to the value found for the circumnuclear diffuse emission. Only in the case in which a single power law is combined with a thermal plasma model (models 2 and 3) did we obtain a better (but still unacceptable) fit compared to the models with solar abundance. In all cases the subsolar abundance resulted in slightly flatter slopes for the power-law components but was still consistent within the errors with those from the fits with solar abundance. We found that altering the assumed abundance of the thermal gas leads to no significant difference in the absorbing column that we infer for the heavily absorbed component. Given the large uncertainties associated with the abundance measurements and the possibility that they are affected by the presence of a power-law component, in our analysis we consider only the results for solar abundance, but our conclusions hold in either case.

As was mentioned in § 2 the observation was performed in 1/2 subarray mode to minimize the effect of pile-up. In order to investigate to what extent our results were affected by pile-up, we fitted the nuclear spectrum with the pile-up model of Davis (2001). Since this model has not been tested for complex spectra, we applied it on the simplest model that reasonably describes the data (model 3). The results from these spectral fits ($kT = 0.41^{+0.02}_{-0.02}$ keV, $\Gamma = -0.04^{+0.04}_{-0.12}$) were consistent with those from fits without the pile-up model, indicating that the effect of pile-up in our spectrum is minimal. Further support for this comes from the low value of the α parameter ($\alpha < 0.078$), which is a measure of the grade migration due to pile-up (Davis 2001). Therefore we conclude that our spectral results are unaffected by pile-up.

3. DISCUSSION

We have found that the nuclear X-ray emission of NGC 4261 can be described by three components: a heavily obscured, flat power law ($\Gamma_1 = 1.54^{+0.71}_{-0.39}$, $N_{\rm H,1} = 8.37^{+3.83}_{-3.03} \times 10^{22}$ cm^{-2}), a less absorbed, steeper power law ($\Gamma_2 = 2.25^{+0.52}_{-0.28}$, $N_{\rm H,2} < 3.7 \times 10^{20}$ cm^{-2}), and a thermal component ($kT = 0.50^{+0.04}_{-0.04}$). These spectral parameters as well as those reported in the rest of this

section are based on model 5 (Tables 2 and 3). We obtain an equally good fit with a single power law ($\Gamma = 1.37^{+0.53}_{-0.37}$) seen through a partially covering absorber ($N_{\rm H} = 7.7^{+3.3}_{-2.7} \times 10^{22}$ cm^{-2}; $f_{\rm cov} = 0.92^{+0.04}_{-0.07}$) plus a thermal plasma component. The following discussion holds for both spectral models. These results are in general agreement with the results from the *XMM-Newton* observation of NGC 4261 (Sambruna et al. 2003). However, the *XMM-Newton* spectrum did not require the second, less obscured power-law component, which is highly significant in our spectral fits. We believe that this is due to the larger beam of *XMM-Newton* ($\sim 10''$ radius) encompassing a larger fraction of the diffuse component, which would mask the weak unobscured power law that is observable only below 2 keV. Although the *XMM-Newton* data provide better constraints than our data on the slope of the obscured power law, in the following discussion we use the results from our spectral fits, which treat the soft and the hard components consistently.

The imaging analysis shows that the emission is extended in the soft band (0.3–2.0 keV), while it is almost pointlike above 4.0 keV. Residuals after subtraction of the nuclear and circumnuclear emission show evidence for an X-ray jet component down to arcsecond scales from the nucleus.

The kinematics of the optically emitting ionized gas in the circumnuclear region indicates the existence of a supermassive black hole ($M_{\rm BH} \sim 4.9 \times 10^8\ M_\odot$). However, there is no clear optical spectral evidence for an AGN (e.g., no broad lines observed either directly or in scattered light; Ho et al. 1997c; Barth et al. 1999). Radio data do show clear evidence for an AGN: NGC 4261 shows prominent jets (see, e.g., Birkinshaw & Davies 1985), while absorption features at their base are interpreted as shadowing by a parsec-scale disk (Jones et al. 2001). In this section, we discuss the nature of the different X-ray spectral components of the nucleus of NGC 4261 and relate them to the multiwavelength observations.

3.1. *The Heavily Obscured Component*

Although the large obscuring column toward the line of sight of the hard component is suggestive of an almost Compton-thick AGN, the lack of a strong Fe Kα line (EW > 1 keV) does not support a reflection-dominated spectrum. On the other hand, the Fe Kα EW expected for transmission of a power-law continuum ($\Gamma \sim 1.2$) through a spherical distribution of gas with the measured equivalent hydrogen column density of $\sim 10^{23}$ cm^{-2} is consistent with the measured upper limit of <590 eV (see, e.g., Makino et al. 1985; Leahy & Creighton 1993).

The best-fit photon index for the highly obscured power-law model is $\Gamma \sim 1.5$, similar to the "canonical" AGN slope of $\Gamma = 1.7$ (see, e.g., Turner et al. 1997). The absorption-corrected luminosity of this component is 2.4×10^{41} ergs s^{-1} (in the 0.1–10.0 keV band), which implies a fraction $\sim 3.9 \times 10^{-6}$ of the Eddington luminosity for a $4.9 \times 10^8\ M_\odot$ black hole (or an accretion rate of $4.3 \times 10^{-6}\ \eta^{-1}\ M_\odot$ yr^{-1}, where η is the accretion efficiency and is expected to be ~ 0.1). Even with a bolometric correction of $L_{\rm X}/L_{\rm bol} \sim 0.2$ (based on the spectral energy distributions of low-luminosity AGNs [LLAGNs]; Ho 1999) the emitted luminosity is only a fraction 2.0×10^{-5} of the Eddington luminosity.

Using the parameters derived for the hot gas in the vicinity of the nucleus (§ 2.2), we estimate, following Di Matteo et al. (2003), the Bondi-Hoyle (Bondi 1952) accretion luminosity to be $L_{\rm B\text{-}H} = \eta 6.2 \times 10^{44}$ ergs for the measured black hole mass of $4.9 \times 10^8\ M_\odot$. The accretion luminosity is a factor of $\sim 2500\eta$ larger than the emitted luminosity of the hard power-law component.

Recent theoretical accretion models suggest that in significantly sub-Eddington accretion rates (which is the case here) the standard geometrically thin/optically thick accretion disks are unstable, and other forms of accretion appear (see, e.g., Frank et al. 2002). These types of accretion, which are radiatively inefficient, have been used to describe the broadband emission of several other LLAGNs (see, e.g., Di Matteo et al. 2000). On the other hand, the existence of strong radio jets down to subparsec scales from the nucleus suggests that the jets could be the origin of the hard X-ray component. We discuss these three possibilities in turn.

1. *Advection-dominated accretion flows (ADAFs).*—ADAFs (Kato et al. 1998; Narayan & Yi 1995) have been the standard model for low radiative efficiency accretion either on their own or as part of a hybrid accretion flow consisting of a truncated standard accretion disk that in its inner part becomes an ADAF (see, e.g., Quataert et al. 1999).

The detection of shadowing of the jet in NGC 4261 strongly supports the case for an accretion disk extending at least 0.2 pc from the black hole but which could be truncated at a smaller radius (Jones et al. 2000, 2001), in agreement with existing hybrid accretion disk models. The measured X-ray spectral index ($\Gamma = \alpha + 1 = 1.54$) is similar to the radio core slope ($\alpha = 0.53$ for a $1\farcs5$–$3\farcs75$ beam; Verdoes Kleijn 2002), indicating that the X-rays could be due to Comptonization of either the accretion disk emission or electron synchrotron emission (synchrotron self-Compton; SSC). Given the intensity of the nuclear X-ray emission, the observed radio emission is much higher than expected from the accretion flow in ADAF models, although this is most probably due to the contribution of the jet. Nonetheless, a truncated accretion disk with an inner ADAF is qualitatively consistent with the current multiwavelength data.

2. *Convection-dominated accretion flow (CDAF).*—This type of accretion flow has been proposed recently, in order to overcome instability problems in ADAFs (Ball et al. 2001). The X-ray spectra predicted by CDAF models for a nucleus with the luminosity of NGC 4261 have $\Gamma \sim 1.8$, steeper than but consistent within the limits with the measured spectrum of the nucleus. However, we note that if the power-law parameters determined from the *XMM-Newton* spectra are not affected by the larger extraction region, the smaller error of the power-law slope given by Sambruna et al. (2003) rules out the CDAF scenario.

The X-ray (1 keV) to radio (4.8 GHz) flux density ratio predicted by CDAF models (Ball et al. 2001) is consistent with the observed ratio [$\log (\nu L_{1\ \rm keV}/\nu L_{4.8\ \rm GHz}) = 1.30$] only for relatively high-viscous heating parameters ($\delta \sim 0.5$) and low accretion rate ($\dot{m} \sim 10^{-6}\ \dot{M}_{\rm Edd}$). Similarly, only these CDAF models have radio to X-ray spectral indices ($0.62 < \alpha_{\rm rx} < 0.96$),[5] consistent with the value we measure for NGC 4261 ($\alpha_{\rm rx} = 0.84$). Since the measured radio emission of NGC 4261 is dominated by the jet, the estimated $\log (\nu L_{\rm X}/\nu L_{\rm rad})$ ratio does not reflect the properties of only the accretion flow, and in this respect should be considered as a lower limit.

3. *Emission from jets.*—Recently Yuan et al. (2002) proposed that the broadband properties of LLAGNs can be explained by emission from jets (e.g., NGC 4258, Yuan et al. 2002; IC 1459, Fabbiano et al. 2003). The detection of a two-sided radio jet in NGC 4261 down to subparsec scales (Jones et al. 2001) suggests that the hard X-ray emission might be related to the jets before they emerge from the obscuring material. This is supported by the similarity between the radio spectral index of the

[5] Defined as $\alpha_{\rm rx} = -\log [f_\nu(1\ \rm keV)/f_\nu(8.4\ \rm GHz)]/7.45$.

jets ($\alpha = 0.29 \pm 0.07$; Piner et al. 2001)[6] and the X-ray photon index ($\Gamma = 1.54^{+0.71}_{-0.39}$). The radio (4.8 GHz) to X-ray spectral index ($\alpha_{rx} = 0.84$) indicates that the spectrum breaks between the radio and X-ray bands. However, the uncertainty on the X-ray spectral index is such that no useful estimate of the break frequency can be made, and it is not possible to distinguish between a synchrotron origin for these X-rays (where, for example, the spectrum might break at about 10^{13} Hz by $\Delta\alpha \approx 1$ to a value consistent with the upper bound of the measured X-ray photon index) or an inverse Compton origin, where the X-ray and radio spectral indices should match (which is consistent with the lower bound of the measured X-ray photon index). It is clear that this component of the X-ray emission could be related to either the large scale or the milliarcsecond-scale VLBI jet, with either a synchrotron or inverse Compton emission mechanism being possible. We note that since the jet is two sided (in both milliarcsecond and arcsecond scales) and so has little relativistic beaming, we would not expect to see significant variability.

3.2. *Obscuration*

An important parameter of the hard power-law component is its large obscuring column density. As is clearly seen in Figure 1, the region from which we extracted the spectrum includes the obscuring dust lane, which might be responsible for the measured X-ray absorption. However, the detection of a nuclear, arcsecond-scale, pointlike source in optical/UV wavelengths (see, e.g., Ferrarese et al. 1996; Jaffe et al. 1996; Chiaberge et al. 2003) indicates that the X-ray absorber has a much smaller scale than the optically emitting region. This is because the X-ray column density, which corresponds to an equivalent extinction of $A_V \sim 36$ mag (from the scaling given by Gorenstein 1975), would totally obscure the nuclear optical/UV light, unless the extinction curve and/or the gas-to-dust ratio differ greatly from those of the Galaxy. The observed nuclear optical/UV emission is thus most probably scattered rather than direct light or is related to the radio jet (after it emerges from the obscuring screen), as discussed by Chiaberge et al. (2003). If, with better astrometry, the 0.″2 offset between the X-ray and optical nuclear sources proved to be real, this would support the latter interpretation for the origin of the optical emission, since the optical emission appears to extend in the direction of the radio jet. Another possibility is that the X-ray absorption is due to warm absorbing material (see, e.g., Brandt et al. 1997). In this case, the gas-to-dust ratio would differ greatly from that in the Galaxy, and it is possible that a significant fraction of the intrinsic UV radiation will not be absorbed.

High-resolution (~20 mas; 3.4 pc) H I observations at 21 cm (van Langevelde et al. 2000) show that the column density toward the core is $<2.2\times10^{18}(T_{sp}/\mathrm{K})$ cm^{-2}, where T_{sp} is the spin temperature of the absorbing gas. An unrealistically high value for the spin temperature, $>10^4$ K, is required to match the H I column density with the N_H inferred from the spectral fits. This indicates that the obscured X-ray component lies on scales much smaller than ~20 mas, and its high N_H is diluted within the radio beam. In fact, based on the estimate of Langevelde et al. (2000) and the detection of a shadow on the counter jet, Jones et al. (2001) give an upper limit of ~4000 Schwarzschild radii on the transition from an optically thick accretion disk to an optically thin accretion flow (e.g., ADAF). This limit, as they point out, is much larger than the radius where the optically thin accretion flow is expected to initiate, allowing for a denser disk on smaller scales, which might be associated with the X-ray emission.

Despite the presence of a UV nuclear component in NGC 4261, its intensity is much lower than would be expected for a typical AGN (see, e.g., the spectral energy distribution of Chiaberge et al. 2003; Ho 1999). These results indicate that absorption of the UV/X-ray emission from the central engine may be partly responsible for the optical properties of LINER galaxies; the absorption alone could account for the lack of a UV bump and broad emission lines, as has been postulated before (Maoz et al. 1995; Pogge et al. 2000). Obscuring material uniformly distributed around the central engine may also explain the weakness of the high-excitation lines, since the ionizing continuum, which is responsible for the optical emission lines, would be significantly attenuated. In this case the commonly used optical line diagnostic diagrams (see, e.g., Veilleux & Osterbrock 1987; Kewley et al. 2001) cannot be used to identify the activity type, since they are based on power-law ionizing continua, which would not be appropriate in the presence of significant extinction.

3.3. *The Unobscured Nuclear Component: A Subarcsecond X-Ray Jet?*

Apart from the heavily absorbed, hard power-law component in the nuclear spectrum, the double power-law model requires a softer ($\Gamma = 2.25^{+0.52}_{-0.28}$) unabsorbed ($N_H < 3.7\times10^{20}$ cm^{-2}) power law. The low absorption and the relatively soft spectrum of this component indicate that it does not originate from the same emitting region as the hard, heavily obscured power law discussed earlier (§ 3.1), nor is it due to scattering of the latter. While the photon index of this component ($\Gamma = 2.25^{+0.52}_{-0.28}$) would be compatible with a population of XRBs, this is unlikely, since a large number (>50) of luminous XRBs ($L_X \sim 5\times10^{38}$) in a small region (of radius ~160 pc) would be required in order to reproduce its intrinsic luminosity. Therefore, we suggest that this X-ray component emanates from the innermost regions of the jet (Fig. 2; § 2.1), as proposed by Worrall & Birkinshaw (1994) based on *ROSAT* data. This connection is supported by the 1 keV flux of this component, which is within a factor of a few of that estimated on the basis of the nuclear 4.8 GHz radio flux, using the X-ray to radio ratio of knot A in the western jet: $f^{obs}_{1\,keV} = 2.4^{+0.95}_{-0.37}\times 10^{-5}$ keV cm^{-2} s^{-1} keV^{-1} versus $f^{est}_{1\,keV} = 8.1\times10^{-6}$ keV cm^{-2} s^{-1} keV^{-1}. Given the strong dependence of the flux density on the details of the electron spectrum, these two estimates are in reasonable agreement. Moreover, based on the difference of the spectral index of this component ($\alpha_X = \Gamma - 1 = 1.25^{+0.52}_{-0.28}$) and the radio index of the nucleus ($\alpha_X \sim 0.50$; Jones et al. 2000), the soft component cannot be the result of inverse Compton scattering of the nuclear emission by the radio-jet electrons. Therefore, the most plausible interpretation for this component is that it is due to synchrotron emission by the jet.

Contrary to Chiaberge et al. (2003), we believe it is likely that this component with low column density is related to the nuclear UV and optical continuum emission. If the obscured power-law component is related to the base of the jet, the steep unobscured power law could be associated with the inner part of the jet after it emerges from the obscuring screen.

A possibility with less physical basis, but which is supported by the similarity (within the errors) between the spectral indices of the obscured and unobscured components, is that they are originating in the same region covered by a "leaky" absorber. In this case based on the ratio of their luminosity, we estimate a covering factor of ~90%.

[6] Here, in contrast to Piner et al. (2001), we follow the $S \propto \nu^{-\alpha}$ definition for the spectral index, for consistency with the notation customarily used for the X-ray photon index $\Gamma = \alpha + 1$.

3.4. *The Diffuse Emission*

As was indicated by fitting the nuclear spectrum, there is a 0.5 keV thermal component that accounts for 80% of the observed soft (0.1–2.0 keV) X-ray emission of the nucleus. The surface brightness profile in this band, presented in Figure 3, shows that this emission is extended.

Based on the existing data for circumnuclear diffuse emission, we cannot discriminate between single-component thermal plasma models with subsolar abundances and thermal plasma/power-law composite models. However, since a power-law component associated with unresolved XRBs is expected, we favor the latter model. In fact, the slope of the power law ($\Gamma = 2.5$) is similar to that observed in galactic discrete sources (see, e.g., Fabbiano 1989; Zezas et al. 2002; Irwin et al. 2003). This power law is seen through progressively lower absorption at larger radii from the nucleus.

Based on the *V*-band radial profile of the galaxy and the relation between *V*-band and X-ray luminosity for XRBs in elliptical galaxies (Kim & Fabbiano 2004; Athey 2003), we find that the estimated total luminosity of an XRB population is in excellent agreement with the observed absorption-corrected luminosity of the power-law component in each bin [$L_X \sim (2\text{–}4) \times 10^{39}$ ergs s^{-1}].

4. IMPLICATIONS FOR THE LINER PHENOMENON AND CONCLUSIONS

We have presented results from a study of the nucleus of the LINER type 2 galaxy NGC 4261, based on a *Chandra* ACIS-S observation. We find that the X-ray spectrum of the nucleus is flat and can be well fitted with a heavily absorbed power law ($\Gamma_1 = 1.54^{+0.71}_{-0.39}$, $N_{\rm H,1} = 8.37^{+3.83}_{-3.03} \times 10^{22}$ cm^{-2}) associated with either the accretion flow or the base of the jet within 20 mas (3.4 pc) from the nucleus, and a softer ($\Gamma_2 = 2.25^{+0.52}_{-0.28}$), less absorbed ($N_{\rm H,2} < 0.037 \times 10^{20}$ cm^{-2}) power law associated with synchrotron radiation from the jet after it emerges from the obscuring screen. The 0.1–10.0 keV luminosity of the heavily absorbed component implies that the accretion rate is a fraction $\sim 10^{-6}$ of the Eddington rate. The multiwavelength data are consistent with ADAF, or jet/disk accretion models, expected to apply in such low accretion regimes.

The results from this study of NGC 4261 indicate that a heavily obscured low luminosity AGN may explain the basic characteristics of at least some type 2 LINERs:

1. Obscuration of the central engine may be responsible for the nondetection of broad lines in the optical spectra of LINERs, as was suggested by Maoz et al. (1995). In this case the observed UV emission could be reprocessed nuclear emission (e.g., by scattering), jet-related emission (see, e.g., Chiaberge et al. 2003), or foreground stellar radiation. In either case we would not expect a strong UV bump. The first two possibilities may apply in NGC 4261, since the absorbing column density for the hard component (equivalent to $A_V \sim 36$ mag) is much higher than that inferred from optical observations ($A_V < 1.0$ mag; Ferrarese et al. 1996), and this discrepancy cannot be explained by any realistic models for non-Galactic gas-to-dust ratios. Foreground star formation is ruled out on the basis of optical spectroscopy.

2. A fully covering absorber situated between the broad- and the narrow-line regions could explain the absence of high-excitation lines in the LINER spectra. In this case the optical line ratios cannot be used as a reliable activity diagnostic, unless the effect of the obscuration on the shape of the photoionizing continuum is taken into account.

3. The detection of radio cores and jets appears to be a common feature in LINERs and LLAGNs in general (see, e.g., Falcke et al. 2000; Ulvestad & Ho 2001). Since some of the observed X-ray emission from the core of NGC 4261 is almost certainly of jet origin, it is possible that it is the source of the UV ionizing continuum. In this case, if the synchrotron spectrum breaks in the optical/UV range, the UV bump would be weak or even absent, resulting in weak or absent high-excitation lines.

4. The presence of a jet may be responsible for the development of shocks in the nuclear and circumnuclear regions of galaxies and therefore may explain the class of LINERs that have optical spectra consistent with shock excitation (see, e.g., Dopita & Sutherland 1996). Recently Kewley et al. (2001) showed that the optical spectra of some LINERs are consistent with shocks in gas-poor environments. All of the LINERs from the work of Nagar et al. (2001, 2002) and Falcke et al. (2000) also have optical spectra consistent with shocks in gas-poor environments, as do the majority of the LINERs from the unbiased sample of Ho et al. (1997b).

The similarity of the intrinsic spectrum of the nucleus of NGC 4261 with the spectrum of the X-ray background suggests that if large enough numbers of such objects exist at higher redshift, they could make a significant contribution to the X-ray background. If such AGNs are associated with spiral galaxies, the lack of broad lines and strong UV continuum in their optical spectra make them good candidates for the emission line galaxies (ELGs) found in the *Chandra* deep surveys. On the other hand, if these AGNs are hosted by early-type galaxies (as is the case for NGC 4261), it is possible that the weak emission lines will be diluted by the much stronger starlight in integrated optical spectra. Thus, for example, an optical spectrum of the NGC 4261 nucleus with even a 2.″5 aperture is typical of early-type galaxies, with only weak Hα and [N II] lines and no Hβ or [O III] emission lines. Such objects would be classified as absorption-line galaxies (ALGs) if observed at the typical brightnesses of the optical counterparts of the deep X-ray survey sources. In fact, in the Chandra Deep Field–North survey (Brandt et al. 2001), 67% and 33% of the X-ray–detected ELGs and ALGs, respectively, are also radio sources (Bauer et al. 2002). However, the stacked X-ray spectra of the ALGs suggest steeper photon indices than observed in NGC 4261.

These results provide evidence that the radio galaxy NGC 4261, which has a LINER type 2 spectrum, has a heavily obscured nucleus. Similar studies of other LINER type 2 AGNs can be used to measure which fraction of them are bona fide AGNs, in order (1) to constrain the demographics of the least luminous (but most numerous; Ho et al. 1997a) AGNs, and (2) to investigate if they can have a significant contribution in the X-ray background.

We would like to thank Aneta Siemiginowska and Fabrizio Nicastro for useful discussions and suggestions. We also would like to thank an anonymous referee for constructive suggestions. We thank the CXC DS and SDS teams for the pipeline reduction of the data and for developing the software used for the pipeline reduction (SDP) and subsequent analysis (CIAO). This work was supported by NASA contract NAS 8-39073 (CXC) and NASA grant G01-2116X. A. P. acknowledges support from the Harvard-Smithsonian Center for Astrophysics Summer Intern Program.

REFERENCES

Alonso-Herrero, A., Rieke, M. J., Rieke, G. H., & Shields, J. C. 2000, ApJ, 530, 688
Athey, A. E. 2003, Ph.D. thesis, Univ. Michigan
Ball, G. H., Narayan, R., & Quataert, E. 2001, ApJ, 552, 221
Barth, A. J., Filippenko, A. V., & Moran, E. C. 1999, ApJ, 525, 673
Bauer, F. E., Alexander, D. M., Brandt, W. N., Hornschemeier, A. E., Vignali, C., Garmire, G. P., & Schneider, D. P. 2002, AJ, 124, 2351
Bevington, P. R., & Robinson, D. K. 1992, Data Reduction and Error Analysis for the Physical Sciences (2nd ed.; New York: McGraw Hill)
Biretta, J., et al. 1997, WFPC2 Instrument Handbook, version 5.0 (Baltimore: STScI), http://www.stsci.edu/instruments/wfpc2/Wfpc2_hand2/wfpc2_inst_hbTOC.html
Birkinshaw, M., & Davies, R. L. 1985, ApJ, 291, 32
Bondi, H. 1952, MNRAS, 112, 195
Brandt, W. N., Mathur, S., Reynolds, C. S., & Elvis, M. 1997, MNRAS, 292, 407
Brandt, W. N., et al. 2001, AJ, 122, 2810
Chiaberge, M., Gilli, R., Macchetto, F. D., Sparks, W. B., & Capetti, A. 2003, ApJ, 582, 645
Colbert, E. J. M., Heckman, T. M., Ptak, A. F., Strickland, D. K., & Weaver, K. A. 2004, ApJ, 602, 231
Davis, D. S., Mushotzky, R. F., Mulchaey, J. S., Worrall, D. M., Birkinshaw, M., & Burstein, D. 1995, ApJ, 444, 582
Davis, J. E. 2001, ApJ, 562, 575
de Vaucouleurs, G., de Vaucouleurs, A., Corwin, H. G., Buta, R. J., Paturel, G., & Fouque, P. 1991, Third Reference Catalogue of Bright Galaxies (Berlin: Springer)
Di Matteo, T., Allen, S. W., Fabian, A. C., Wilson, A. S., & Young, A. J. 2003, ApJ, 582, 133
Di Matteo, T., Quataert, E., Allen, S. W., Narayan, R., & Fabian, A. C. 2000, MNRAS, 311, 507
Dopita, M. A., Koratkar, A. P., Allen, M. G., Tsvetanov, Z. I., Ford, H. C., Bicknell, G. V., & Sutherland, R. S. 1997, ApJ, 490, 202
Dopita, M. A., Koratkar, A. P., Evans, I. N., Allen, M., Bicknell, G. V., Sutherland, R. S., Hawley, J. F., & Sadler, E. 1996, in ASP Conf. Ser. 103, The Physics of LINERs in View of Recent Observations, ed. M. Eracleous et al. (San Francisco: ASP), 44
Dopita, M. A., & Sutherland, R. S. 1996, ApJS, 102, 161
Eracleous, M., Shields, J. C., Chartas, G., & Moran, E. C. 2002, ApJ, 565, 108
Fabbiano, G. 1989, ARA&A, 27, 87
Fabbiano, G., Kim, D.-W., & Trinchieri, G. 1992, ApJS, 80, 531
Fabbiano, G., et al. 2003, ApJ, 588, 175
Falcke, H., Nagar, N. M., Wilson, A. S., & Ulvestad, J. S. 2000, ApJ, 542, 197
Ferrarese, L., Ford, H. C., & Jaffe, W. 1996, ApJ, 470, 444
Filippenko, A. V. 1996, in ASP Conf. Ser. 103, The Physics of LINERs in View of Recent Observations, ed. M. Eracleous et al. (San Francisco: ASP), 17
Filippenko, A. V., & Terlevich, R. 1992, ApJ, 397, L79
Frank, J., King A. R., & Raine, D. J. 2002, Accretion Power in Astrophysics (3rd ed.; Cambridge: Cambridge Univ. Press)
Garmire, G. P. 1997, BAAS, 29, 823
Georgantopoulos, I., Panessa, F., Akylas, A., Zezas, A., Cappi, M., & Comastri, A. 2002, A&A, 386, 60
Gliozzi, M., Sambruna, R. M., & Brandt, W. N. 2003, A&A, 408, 949
Gorenstein, P. 1975, ApJ, 198, 95
Heckman, T. M. 1980, A&A, 87, 152
Ho, L. C. 1999, ApJ, 516, 672
Ho, L. C., Filippenko, A. V., & Sargent, W. L. W. 1997a, ApJ, 487, 568
———. 1997b, ApJS, 112, 315
Ho, L. C., Filippenko, A. V., Sargent, W. L. W., & Peng, C. Y. 1997c, ApJS, 112, 391
Ho, L. C., et al. 2001, ApJ, 549, L51
Imanishi, M., Dudley, C. C., & Maloney, P. R. 2001, ApJ, 558, L93
Irwin, J. A., Athey, A. E., & Bregman, J. N. 2003, ApJ, 587, 356
Jaffe, W., Ford, H. C., Ferrarese, L., van den Bosch, F., & O'Connell, R. W. 1993, Nature, 364, 213
———. 1996, ApJ, 460, 214
Jones, D. L., Wehrle, A. E., Meier, D. L., & Piner, B. G. 2000, ApJ, 534, 165
Jones, D. L., Wehrle, A. E., Piner, B. G., & Meier, D. L. 2001, ApJ, 553, 968
Kato, S., Fukue, J., & Mineshige, S. 1998, Black Hole Accretion Disks, ed. S. Kato, J. Fukue, & S. Mineshige (Kyoto: Kyoto Univ. Press)
Kewley, L. J., Heisler, C. A., Dopita, M. A., & Lumsden, S. 2001, ApJS, 132, 37
Kim, D., & Fabbiano, G. 2003, ApJ, 586, 826
———. 2004, ApJ, 611, 846
Leahy, D. A., & Creighton, J. 1993, MNRAS, 263, 314
Magdziarz, P., & Zdziarski, A. A. 1995, MNRAS, 273, 837
Makino, F., Leahy, D. A., & Kawai, N. 1985, Space Sci. Rev., 40, 421
Maoz, D., Filippenko, A. V., Ho, L. C., Rix, H., Bahcall, J. N., Schneider, D. P., & Macchetto, F. D. 1995, ApJ, 440, 91
Marshall, H. L., Tennant, A., Grant, C. E., Hitchcock, A. P., O'Dell, S. L., & Plucinsky, P. P. 2004, Proc. SPIE, 5165, 497
Matsumoto, Y., Fukazawa, Y., Nakazawa, K., Iyomoto, N., & Makishima, K. 2001, PASJ, 53, 475
Matsushita, K., Ohashi, T., & Makishima, K. 2000, PASJ, 52, 685
Matt, G., Fabian, A. C., Guainazzi, M., Iwasawa, K., Bassani, L., & Malaguti, G. 2000, MNRAS, 318, 173
Nagar, N. M., Falcke, H., Wilson, A. S., & Ulvestad, J. S. 2002, A&A, 392, 53
Nagar, N. M., Wilson, A. S., & Falcke, H. 2001, ApJ, 559, L87
Nandra, K., George, I. M., Mushotzky, R. F., Turner, T. J., & Yaqoob, T. 1997, ApJ, 476, 70
Narayan, R., & Yi, I. 1995, ApJ, 452, 710
Pellegrini, S., Fabbiano, G., Fiore, F., Trinchieri, G., & Antonelli, A. 2002, A&A, 383, 1
Piner, B. G., Jones, D. L., & Wehrle, A. E. 2001, AJ, 122, 2954
Pogge, R. W., Maoz, D., Ho, L. C., & Eracleous, M. 2000, ApJ, 532, 323
Quataert, E., di Matteo, T., Narayan, R., & Ho, L. C. 1999, ApJ, 525, L89
Raymond, J. C., & Smith, B. W. 1977, ApJS, 35, 419
Sambruna, R. M., Gliozzi, M., Eracleous, M., Brandt, W. N., & Mushotzky, R. 2003, ApJ, 586, L37
Taniguchi, Y., Shioya, Y., & Murayama, T. 2000, AJ, 120, 1265
Terashima, Y., Ho, L. C., Ptak, A. F., Mushotzky, R. F., Serlemitsos, P. J., Yaqoob, T., & Kunieda, H. 2000, ApJ, 533, 729
Terashima, Y., Iyomoto, N., Ho, L. C., & Ptak, A. F. 2002, ApJS, 139, 1
Turner, T. J., George, I. M., Nandra, K., & Mushotzky, R. F. 1997, ApJS, 113, 23
Ulvestad, J. S., & Ho, L. C. 2001, ApJ, 562, L133
van Langevelde, H. J., Pihlström, Y. M., Conway, J. E., Jaffe, W., & Schilizzi, R. T. 2000, A&A, 354, L45
Veilleux, S., & Osterbrock, D. E. 1987, ApJS, 63, 295
Verdoes Kleijn, G. A., Baum, S. A., de Zeeuw, P. T., & O'Dea, C. P. 2002, AJ, 123, 1334
Weisskopf, M., Tananbaum, H., Van Speybroeck, L., & O'Dell, S. 2000, Proc. SPIE, 4012, 2
Worrall, D. M., & Birkinshaw, M. 1994, ApJ, 427, 134
Xu, H., et al. 2002, ApJ, 579, 600
Yuan, F., Markoff, S., Falcke, H., & Biermann, P. L. 2002, A&A, 391, 139
Zezas, A., Fabbiano, G., Rots, A. H., & Murray, S. S. 2002, ApJ, 577, 710